*3094–3105* *Nucleic Acids Research, 2010, Vol. 38, No. 9* *Published online 27 January 2010*
*doi:10.1093/nar/gkp1253*

# Binding of aminoglycoside antibiotics to helix 69 of 23S rRNA

**Ann E. Scheunemann, William D. Graham, Franck A. P. Vendeix and Paul F. Agris***

Department of Molecular and Structural Biochemistry, North Carolina State University, Raleigh, NC 27695-7622, USA

Received October 26, 2009; Revised and Accepted December 29, 2009

## ABSTRACT

**Aminoglycosides antibiotics negate dissociation and recycling of the bacterial ribosome's subunits by binding to Helix 69 (H69) of 23S rRNA. The differential binding of various aminoglycosides to the chemically synthesized terminal domains of the *Escherichia coli* and human H69 has been characterized using spectroscopy, calorimetry and NMR. The unmodified *E. coli* H69 hairpin exhibited a significantly higher affinity for neomycin B and tobramycin than for paromomycin ($K_d$s = 0.3 ± 0.1, 0.2 ± 0.2 and 5.4 ± 1.1 μM, respectively). The binding of streptomycin was too weak to assess. In contrast to the *E. coli* H69, the human 28S rRNA H69 had a considerable decrease in affinity for the antibiotics, an important validation of the bacterial target. The three conserved pseudouridine modifications (Ψ1911, Ψ1915, Ψ1917) occurring in the loop of the *E. coli* H69 affected the dissociation constant, but not the stoichiometry for the binding of paromomycin ($K_d$ = 2.6 ± 0.1 μM). G1906 and G1921, observed by NMR spectrometry, figured predominantly in the aminoglycoside binding to H69. The higher affinity of the *E. coli* H69 for neomycin B and tobramycin, as compared to paromomycin and streptomycin, indicates differences in the efficacy of the aminoglycosides.**

## INTRODUCTION

The 2-deoxystreptamine (2-DOS) aminoglycosides (Figure 1) are a group of broad spectrum antibiotics known to interact with the prokaryotic ribosome's 16S rRNA in the small (30S) subunit, specifically with the helix 44 (h44) decoding or A-site (1,2). Though aminoglycoside binding of the A-site has become a model of the antibiotic's class action (3), aminoglycosides also bind to the large (50S) subunit of the ribosome (4,5), and to other RNAs to varying degrees. Other RNAs studied for their binding of aminoglycosides include the *trans*-activating region (TAR) and the Rev protein response element (RRE) RNA of the human immunodeficiency virus, ribozymes, aptamers and the human tau protein RNA regulatory element (6–8). Binding properties of the aminoglycoside are dependent on the nature of the particular aminoglycoside and the target RNA. However, as a class the aminoglycosides appear to bind to unequal, internal loops, to hairpin loops and to A-minor motifs. The neomycin-class of aminoglycosides are related by their ringed structures, neamine, present in all 4,5 2-DOS linked families (Figure 1C and D). Rings I and II bind to the A-site of the bacterial ribosome's small subunit and cause tRNA to misread mRNA codons (9). Individual $H_2O$ molecules affect the manner in which the different aminoglycosides bind at the A-site by altering the conformation of the binding site and changing the structure of the aminoglycosides (10–12). Though their chemical structures differ, the affinities of the aminoglycosides for the bacterial ribosome's A-site are similar. The binding affinities of the aminoglycosides are related to the number of hydrogen bonds between the aminoglycosides and the RNA, whether bound directly or water mediated (12,13). Paromomycin (Figure 1E) binds in a deep groove of the 16S rRNA facilitated by direct and water-mediated hydrogen bonds and causes the nucleosides A1492 and A1493 to bulge out of conformation (10–12). Paromomycin also binds in the shallow groove with another $H_2O$ molecule. The shallow groove $H_2O$ is observed in the binding of tobramycin (Figure 1D), but not with geneticin (G-418) (14). Ring III of both tobramycin and geneticin displaces the $H_2O$ molecule

*To whom correspondence should be addressed. Tel: +1-919-515-6188; Fax: +1-919-515-2047; Email: paul_agris@ncsu.edu
Present address:
Franck A.P. Vendeix, Sirga Advanced Biopharma, Inc., 2 Davis Drive, Research Triangle Park, NC 27709, USA.

The authors wish it to be known that, in their opinion, the first two authors should be regarded as joint first authors.

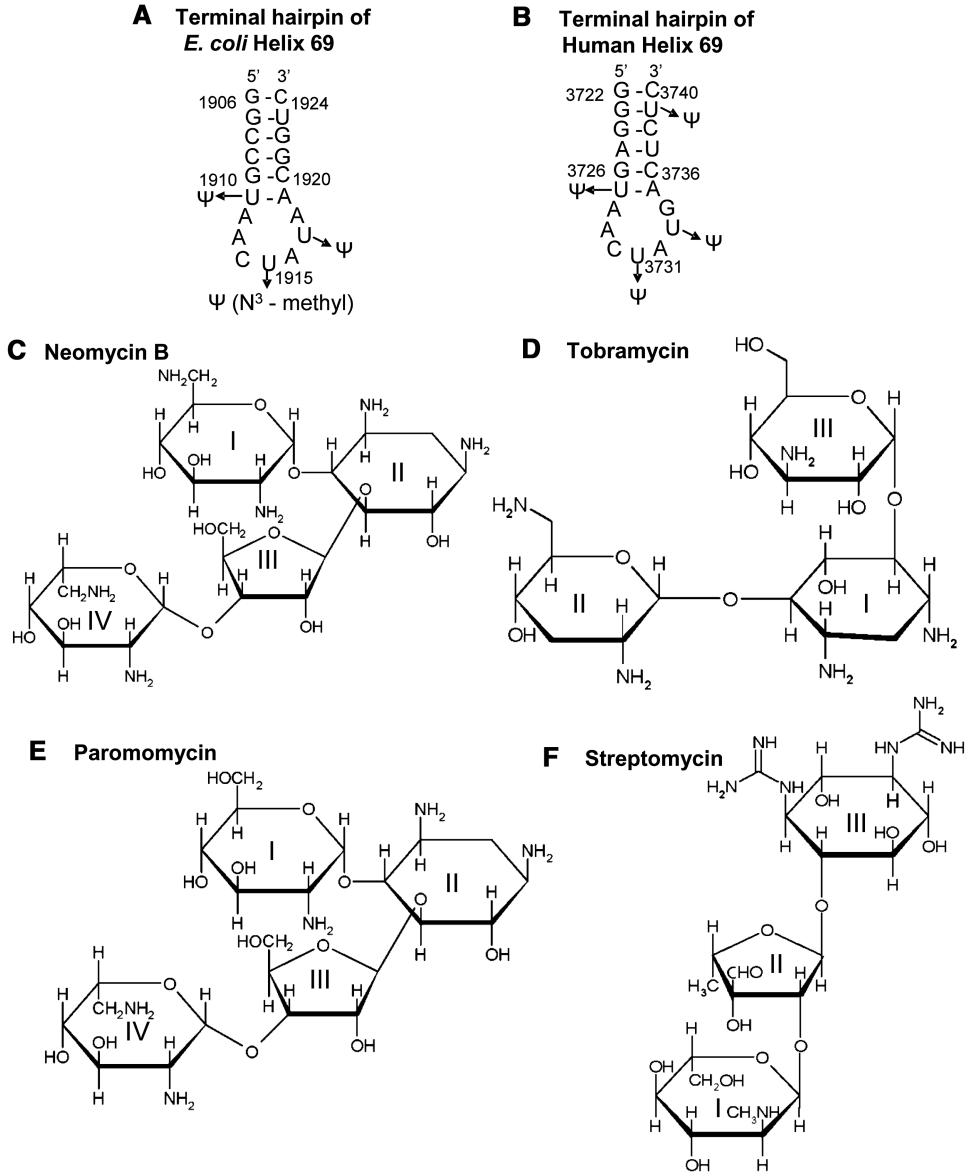


**Figure 1.** Structures of the terminal stems and loops of the *E. coli* and human helix 69, and of the aminoglycosides. (**A**) Terminal hairpin sequence and secondary structure of helix 69 (H69) from the *E. coli* ribosome. The RNA was synthesized with and without the pseudouridine (Ψ) modifications at the 23S rRNA positions of 1911, 1915 and 1917. (**B**) Terminal hairpin sequence and secondary structure of helix 69 from the human ribosome. The RNA was synthesized without the pseudouridine (Ψ) modifications which occur naturally at the 28S rRNA positions of 3727, 3731 3733, 3737 and 3739. The chemical structures of the aminoglycosides used in the reported experiments: (**C**) Neomycin B; (**D**) Tobramycin; (**E**) Paromomycin; (**F**) Streptomycin.

found to be important for paromomycin binding in the deep groove (12,14,15).

Aminoglycosides bind to the ribosome's large subunit, as well as to the small subunit (15–17). The normal dissociation and recycling of the ribosomal subunits are affected by the binding of these antibiotics to Helix 69 (H69) of the large subunit (15). H69 interacts with h44 of the small subunit at the interface of the two subunits (18–20). The contacts between H69 and h44 are similar to an A-minor interaction (21). This interaction may affect the efficiency and accuracy of specific steps in translation (22–25). Ribosome recycling factor (RRF) in conjunction with elongation factor G normally dissolves the H69-h44 interaction and thus, dissociates the subunits. However, the binding of the aminoglycosides to H69 restores the structural contacts between the large and small subunits negating the recycling of the ribosome (15).

A structural study has detailed the binding of the aminoglycosides neomycin B (Figure 1C) and gentamicin to the 50S subunit. The aminoglycosides bind the 23S rRNA within the major groove of H69 on the 3′-side of the stem at its junction with the terminal loop and include binding to G1921, U1923 and G1906 (Figure 1A) (15). Aminoglycoside rings I and II may play a role in the binding of the antibiotics to H69, as they do in its

binding to h44. The A-platform seen at the bacterial decoding site is also found in the terminal hairpin of H69 (Figure 1A and B), but is not directly involved in the binding of aminoglycosides to the 23S rRNA. This hairpin is highly conserved, and post-transcriptionally modified with pseudouridines (Ψ). The human H69 hairpin is also modified with the three Ψs, but a G3734 replaces A1918 that is located in the loop of *Escherichia coli* H69 (Figure 1A and B).

We postulated that aminoglycoside antibiotics would bind to a model RNA structure of the unmodified H69 stem and loop, and that specific aminoglycosides would have differential affinities for the RNA. In addition, we postulated that the extensive natural Ψ modifications were perhaps important, but not necessary to the binding affinities of the aminoglycosides. The human H69 sequence has a G3734 at the position analogous to A1918 of the *E. coli* H69 (Figure 1). This difference between the human and bacterial H69 is comparable to the difference between the human and bacterial h44 decoding sites in which a G substitutes for A1408 (26). Because the human h44 has significantly reduced affinity for aminoglycosides in comparison to the *E. coli* h44 (27), we believed that whatever aminoglycoside binding occurred with the *E. coli* H69, its affinity would be reduced with the human RNA sequence. Here we report that the unmodified *E. coli* H69 stem- and loop-domain binds neomycin B, tobramycin and paromomycin, but not streptomycin, with high affinity and that H69 G1906 and G1921 are involved in the binding of the aminoglycosides. The presence of the three almost universally conserved Ψ modifications in the loop of the bacterial H69 hairpin results in a higher affinity of paromomycin. However, a considerable decrease in aminoglycoside affinity was observed for the unmodified human H69 sequence in comparison to the modified and unmodified *E. coli* sequences.

## MATERIALS AND METHODS

### RNA synthesis and purification

RNAs corresponding to nucleosides 1906–1924 of the stem and terminal loop of *E. coli* 23S rRNA Helix 69 (H69) were chemically synthesized (Dharmacon RNA Technologies, CO) with and without the three pseudouridine modifications (Ψ) that occur at positions 1911, 1915 and 1917 (Figure 1A). In addition, the RNA corresponding to nucleosides 3722–3740 of the stem and terminal loop of the human 28S rRNA H69 was chemically synthesized without the modifications. The RNAs were deprotected as suggested by the manufacturer, lyophilized and dissolved in $H_2O$. The RNAs were purified by ion exchange HPLC (28), and concentrations determined by UV absorbance at 260 nm at room temperature (29). The base-paired secondary-structure of the unmodified *E. coli* H69 hairpin was found by nuclear magnetic resonance (NMR) to be similar to that previously reported (21,30,31).

### Aminoglycoside binding determined by UV-monitored thermal denaturations

The H69 samples were dissolved to obtain a concentration of 1 μM in cacodylate buffer (sodium cacodylate, 10 mM; NaCl, 51.5 mM; EDTA, 0.1 mM; pH 6.0). H69 RNA samples were titrated with an aminoglycoside in concentrations from 0 to 10 μM. Thermal denaturations and renaturations were monitored by measuring UV absorbance (260 nm) using a Varian Cary 3 spectrophotometer as published (23,24,32,33). The data points were averaged over 20 s and collected three times a minute with a temperature change of 1°C per minute from 5 to 95°C. Thermal denaturations and renaturations were repeated three times at each concentration of aminoglycoside and conducted on three or four different days providing nine or 12 sets of data from which a point-by-point average of the thermodynamic profile was obtained. The 'melting' temperature ($T_m$) varied by no more than ±0.5°C. The UV data were analyzed as described (32,34,35) and the thermodynamic parameters were determined by using Meltwin (35). The binding of each aminoglycoside to each H69 domain was determined by plotting the change in $T_m$ with increasing concentration of the aminoglycoside. Line fitting analyses using a non-linear regression with a two-site binding were conducted with Prism (GraphPad) from which the dissociation constants ($K_d$) were extracted. The Gibb's free energy of binding ($\Delta G^\circ$) was determined for a temperature of 37°C and from the relationship of the equilibrium binding constant to the free energy, $\Delta G^\circ_{37} = -RT \ln K_{eq}$.

### Circular dichroism spectrapolarimetry and aminoglycoside binding

Circular dichroism (CD) spectra were recorded at 4°C using a Jasco J600 spectrapolarimeter and an interfaced computer (36,37). A jacketed, cylindrical sample cell with a 1 cm light path, was used. RNA sample concentrations were adjusted with cacodylate buffer to ~0.2 absorbance units at 260 nm. H69 RNA samples were titrated with an aminoglycoside to final concentrations of 0, 0.75, 1.50, 2.25, 3.00, 4.50, 5.25, 6.00, 6.75, 7.50, 8.25 and 9.00 μM. CD data are baseline corrected for signals due to the cell, buffer and aminoglycoside. Changes in ellipticity at 262 nm with increases in aminoglycoside were used to generate binding curves from which the dissociation constants were extracted using a non-linear regression analysis with a two-site binding (Prism, GraphPad).

### Isothermal titration calorimetry

Isothermal titration calorimetry (ITC) (38) was conducted at 37°C to determine the binding constants and thermodynamic parameters for aminoglycoside interaction with the unmodified *E. coli* and human H69 RNA hairpins. The H69 samples (40 μM in cacodylate buffer) were titrated with 10 μl aliquots of an aminoglycoside solution (250 μM in cacodylate buffer). Experimental data was corrected for contributions of buffer by subtraction of a titration of the RNA with buffer alone. The change in heat capacity with increasing concentration of

aminoglycoside was analyzed using a non-linear regression with a two-site binding (Prism, GraphPad).

### NMR spectrometry

The $^{1}H$ 1D and 2D NMR spectra were acquired on a Bruker DRX500 spectrometer (NCSU NMR Facility) and processed with either XWINNMR (BrukerBiospin Inc., Rheinstetten, Germany) or NMRPipe (39) and the analyses were achieved with SPARKY (40) or ACD-NMR (41). Since the NMR samples were dissolved in $^{1}H_2O$, the WATERGATE (42) method was used to suppress the water signal. $^{1}H$ 1D NOE difference (43) and 2D NOESY (44,45) experiments of the samples in $^{1}H_2O$ were conducted with mixing times of 50 and 250 ms, respectively, and performed at low temperature (2°C) to observe the exchangeable proton resonances. The titration of *E. coli* unmodified H69 with neomycin B was followed by recording 1D $^{1}H$ spectra. NMR samples of the RNA were 0.3–0.6 mM in 300 µL in 90% $^{1}H_2O$, 10% $^{2}H_2O$, 20 mM phosphate buffer (pH = 6.2), 50 mM $Na^+$ and 50 mM $K^+$. Neomycin B (was in $^{1}H_2O$ solution containing 20 mM phosphate buffer (pH = 6.2), 50 mM $Na^+$ and 50 mM $K^+$. Titrations were performed by direct addition of small aliquots of neomycin (by using micro pipettes) to the NMR tube containing the RNA. All NMR titration experiments were carried out at 2°C.

## RESULTS

### Characterization of the terminal hairpin constructs of H69

The terminal hairpin of the *E. coli* 23S rRNA H69 (nucleosides 1906–1924) was chemically synthesized with and without the three conserved Ψ modifications at positions 1911, 1915 and 1917. The corresponding unmodified human sequence of H69 was chemically synthesized from nucleosides 3722 to 3740 (Figure 1A and B). All three RNAs were purified to homogeneity using HPLC. The three hairpins behaved as unimolecular species when thermally denaturated and renaturated under conditions of moderate ionic strength and pH (cacodylate buffer, pH 6.0). The RNAs exhibited a major helix to random coil transition between the temperatures of 50 and 70°C in the absence of aminoglycosides (Figure 2 and Table 1). The human H69, which has two A•U base pairs in the stem, as opposed to the one for *E. coli* H69, exhibited the lowest of the $T_m$, 52.9°C (Table 1). The three conserved Ψs increased the stability of the *E. coli* H69 hairpin ($\Delta T_m = 1.5$°C), and that of the human H69 hairpin (30,31). The unmodified *E. coli* H69 hairpin exhibited a minor thermal transition, as had been reported by others for the Ψ1911-modified, *E. coli* H69 and the unmodified human H69 (30,31). The minor transition occurred at a temperature below 30°C, under the solution conditions we had used, but was not observed with the modified *E. coli* H69 domain with all three Ψs (Figure 2). Thus, the low-temperature transition could be attributed to the thermal denaturation of the unmodified loop nucleosides that, when modestly stabilized by the modifications, cooperatively melts with the major transition. Pseudouridines on the 3′-side of stems and adjacent to loops, in particular position 39 in the anticodon stem of tRNAs, are known to stabilize the hairpins (33,46), as is position 1911 of H69 (47). Ψ contributes little to thermal stability of tRNA's canonical TΨC loop (48). As observed here (Table 1) and by others (30,31), Ψ does not appear to contribute to the thermal stability of the H69 loop, but does stack with adjacent nucleoside in the H69 loop (47).

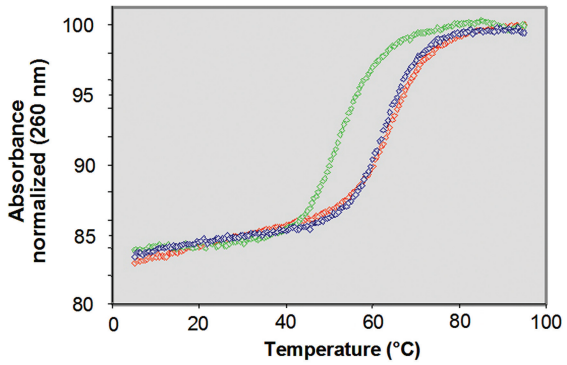


**Figure 2.** Thermal denaturations of the unmodified and modified *E. coli* H69 and the human H69. The unmodified (blue) and modified (red) *E. coli* H69 and the human H69 (green) RNA hairpins were subjected to repeated thermal denaturations and renaturations in the absence of aminoglycosides. The graphs are the results of point-by-point averages of nine transitions. The thermodynamic parameters obtained from the curves are found in Table 1.

**Table 1.** Thermodynamic parameters of the unmodified and Ψ-modified *E. coli* H69 hairpins and the unmodified human H69 hairpin

| Helix 69T | Thermodynamic parameter | | | |
|---|---|---|---|---|
| | $T_m$ (°C)[a] | $\Delta G^\circ$ (kcal/mol) | $\Delta H$ (kcal/mol) | $\Delta S$ (cal/K mol) |
| Modified *E. coli* | 64.7 | −4.5 ± 0.2 | −54.8 ± 5.0 | −126.2 ± 9.6 |
| Unmodified *E. coli* | 63.2 | −4.4 ± 0.2 | −56.7 ± 3.9 | −168.6 ± 15.1 |
| Unmodified human | 52.9 | −2.2 ± 0.1 | −45.9 ± 3.6 | −140.7 ± 11.2 |

[a]$T_m$ values from 9 or 12 determinations varied by ±0.5°C.

### Aminoglycoside binding by *E. coli* H69 and human H69 assessed by UV analyses

The ability of the unmodified and Ψ-modified *E. coli* H69 hairpins, and the unmodified human H69 sequence to bind the aminoglycoside antibiotics, neomycin B, tobramycin, paromomycin and streptomycin (Figure 1 and Supplementary Figures S1 and S2), was assessed by monitoring changes in the major, UV-monitored, thermal transitions, CD ellipticity and ITC of the RNAs when titrated with the aminoglycosides. The binding of aminoglycosides to a model RNA duplex of the decoding site of h44 increased the thermal stability of that RNA (49). With one exception, the binding of aminoglycosides by the modified and unmodified *E. coli* Helix 69, as well as the human H69, exhibited an increase in the $T_m$ of the major thermal transition, as demonstrated by the unmodified *E. coli* H69 bound by neomycin

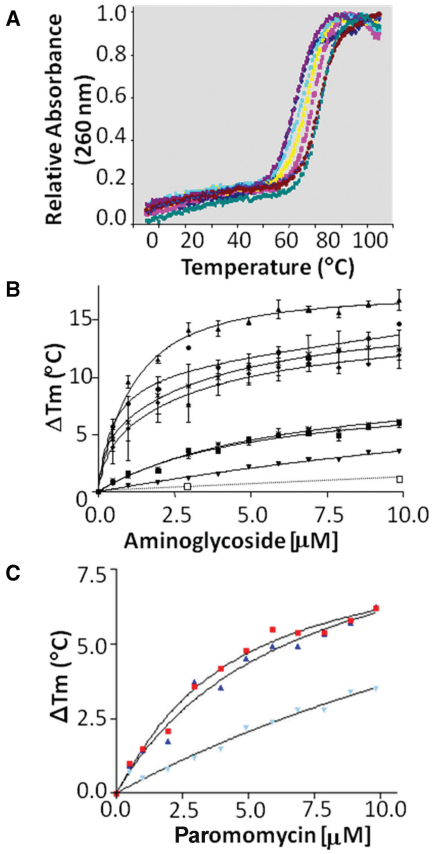


**Figure 3.** (**A**) Effect of neomycin B on the thermal stability of the unmodified *E. coli* H69. The unmodified *E. coli* H69 (1 μM) was titrated with increasing amounts of neomycin B (0–10 μM) and the complex RNA–neomycin B subjected to repeated thermal denaturations and renaturations. Each curve is the result of point-by-point averages of either nine or 12 transitions for each concentration: 0 μM (blue square), 0.75 μM (purple square), 1.50 μM (aqua square), 2.25 μM (yellow triangle), 3.00 μM (pink square), 4.50 μM (dark red circle), 5.25 μM (dark red square), 6.75 μM (small blue square) and 9.00 μM (dark cyan square). With increasing amounts of aminoglycoside, the $T_m$ of the RNA increases. (**B**) Binding of neomycin B, tobramycin, paromomycin and streptomycin to the unmodified *E. coli* H69 and to the human H69. The differences in melting temperature ($\Delta T_m$) of the H69 with the addition of increasing concentrations of aminoglycoside provided binding curves for each of the aminoglycosides. Tobramycin bound to the unmodified *E. coli* H69 (filled triangle) and to the human H69 (cross mark); neomycin bound to the unmodified *E. coli* H69 (filled circle) and to the human H69 (filled rhombus); paromomycin bound to the unmodified *E. coli* H69 (filled square) and to the unmodified human H69 (inverted filled triangle). Streptomycin was not bound by the unmodified *E. coli* H69 and thus, was assessed at two concentrations only (open square). The binding of paromomycin to the Ψ-modified *E. coli* H69 is also shown (double dagger). Addition of streptomycin did not increase the $T_m$. The binding affinities ($K_d$) and free energy of binding ($\Delta G^\circ$) for each aminoglycoside and for the different H69 are shown in Table 2. (**C**) The binding of paromomycin to the unmodified and Ψ-modified *E. coli* H69 and human H69. The unmodified (red square) and Ψ-modified (blue triangle) *E. coli* and human H69 (light-blue inverted triangle) (1 μM) were titrated with paromomycin (0–10 μM) and the RNA was thermally denatured and renatured, repeatedly. Binding curves were extracted from the differences in melting temperature ($\Delta T_m$) of the two H69 RNAs with the addition of increasing concentrations of aminoglycoside. The binding affinities ($K_d$) and free energy of binding ($\Delta G^\circ$) paromomycin by the unmodified and Ψ-modified *E. coli* H69 are shown in Table 2.

(Figure 3A). When titrated with streptomycin, none of the H69 RNAs exhibited increases in $T_m$, or changes in the melting profile (Figure 3B). We concluded that streptomycin did not bind to the H69 RNAs models that we constructed. In contrast when titrated with neomycin B, tobramycin or paromomycin, the UV-monitored denaturations of the unmodified *E. coli* H69 hairpin were significantly altered (Figure 3B). The three antibiotics differentially affected the $T_m$, suggesting that each antibiotic varied in its ability to restructure the unmodified *E. coli* H69 hairpin. Increases in $T_m$ were most readily effected by tobramycin and neomycin B, and less so by paromomycin, indicating a difference in their binding affinities for the RNA. Analysis of the melting data (Figure 3B) using non-linear regression produced binding curves in which the dissociation constant ($K_d$) for each antibiotic could be calculated. The resulting data illustrated that tobramycin was bound to the unmodified hairpin loop of *E. coli* H69 with a $K_d$ of $0.2 \pm 0.2$ μM. Neomycin B and paromomycin also were bound strongly with $K_d$ values of $0.3 \pm 0.1$ and $5.4 \pm 1.1$ μM, respectively (Table 2).

The introduction of the Ψ modification at the loop positions 1911, 1915 and 1917 of the *E. coli* H69 hairpin resulted in an increased affinity of the RNA for the antibiotic. Paromomycin was bound by both the unmodified *E. coli* H69 hairpin and its Ψ-modified counterpart. However, the binding curves (Figure 3C) and the $K_d$s (Table 2) indicated that the presence of modifications increased the association of paromomycin by a factor of two. The modified H69 bound paromomycin with a $K_d$ of $2.6 \pm 0.1$ μM, whereas that of the unmodified RNA was $5.4 \pm 1.1$ μM. The three antibiotics also exhibited differences in their binding affinities for the unmodified human H69 hairpin. Again tobramycin was bound with the highest affinity followed by neomycin B, and finally paromomycin with considerably less affinity (Table 2). Importantly, the three antibiotics were bound by the human H69 hairpin with affinities that were far less than that of the *E. coli* H69. The affinity of the unmodified *E. coli* H69 domain for the antibiotics was as much as 5-fold higher than that of the unmodified human H69. Thus, neomycin B, tobramycin and paromomycin differentially bound the *E. coli* H69 hairpin, and did so with consistently higher affinities than with the human H69.

The data collected from the aminoglycosides binding to the *E. coli* and human H69 constructs corresponded best to non-linear, two-site interactions (Figure 3B). The binding of aminoglycosides to other model RNA systems also have been found to exhibit a better fit with a two-site analysis (50). Each of the aminoglycosides exhibited a significantly higher affinity for the primary binding site than the secondary site (Table 2). Neomycin B and tobramycin exhibited larger difference in affinity between the two sites than did paromomycin for which the $K_d$s doubled. In fact, the second site binding of tobramycin was too weak to be analyzed. The Gibb's free energy of binding ($\Delta G^\circ$) was calculated from the binding constant for the primary- and secondary-site interactions of each of the aminoglycosides with the H69

**Table 2.** Binding of aminoglycoside antibiotics to *E. coli* and human helix 69

| Helix 69 construct and aminoglycoside | $K_d$ (μM) | | $\Delta G_{37}^\circ$ (kcal/mol) | |
|---|---|---|---|---|
| | Site 1 | Site 2 | Site 1 | Site 2 |
| Modified *E. coli* Helix 69 + Paromomycin | 2.6 ± 0.1 | 4.9 ± 0.3 | −7.9 | −7.5 |
| Unmodified *E. coli* Helix 69 + Paromomycin | 5.4 ± 1.1 | 6.4 ± 0.9 | −7.5 | −7.4 |
| Unmodified *E. coli* Helix 69 + Neomycin B | 0.3 ± 0.1 | 4.3 ± 0.7 | −9.3 | −7.6 |
| Unmodified *E. coli* Helix 69 + Tobramycin | 0.2 ± 0.2 | 4.5 ± 0.3 | −9.5 | −7.6 |
| Unmodified Human 69 + Paromomycin | 18.4 ± 1.7 | 35.6 ± 1.1 | −6.7 | −6.3 |
| Unmodified Human 69 + Neomycin B | 1.5 ± 0.3 | 3.7 ± 0.1 | −8.2 | −7.7 |
| Unmodified Human 69 + Tobramycin | 0.5 ± 0.1 | N/A | −9.0 | N/A |

samples. The difference in free energy between the binding of paromomycin to the modified and unmodified *E. coli* H69 was found to be inconsequential (Table 2). However, the differences in free energy between neomycin B and tobramycin binding to the unmodified *E. coli* H69 and that of the paromomycin were considerable ($\Delta\Delta G^\circ \sim 2$ kcal/mol) (Table 2). Differences in free energy for each aminoglycoside binding to the unmodified *E. coli* when compared to the same antibiotic binding to the human H69 hairpin were less ($\Delta\Delta G^\circ \sim 1$ kcal/mol). A Hill analysis was applied to what appeared as a two-site binding of paromomycin to all three RNAs (Supplementary Figure S3). The two-site line fitting analysis of the melting profiles, and the Hill coefficients ($n$) derived from the Hill plot being >1, suggested a modest positive cooperativity in the binding of the paromomycin to the RNA. The coefficient for the unmodified H69 was equivalent to that of the modified H69 ($n$ = 1.53 and 1.48), within error (±0.05). However, the human H69 hairpin had a significantly lower coefficient, 1.33.

## Aminoglycoside binding observed by CD

CD spectropolarimetry of RNA detects changes in base stacking throughout the RNA, stems and loops with changes in solution conditions, modification and the binding of ligands (51,52). CD has the advantage that many interacting small compounds, including ions, and even peptides and proteins exhibit spectral nulls at the wavelengths that RNA demonstrates the largest ellipticity 250–290 nm (52–54). Though we had not tested the affect of changing ionic conditions on aminoglycoside binding to H69, the structure of a human H69 construct was little affected by the addition of $MgCl_2$ (31). The CD experiments were performed to confirm the data collected from the UV-monitored thermal transitions of the unmodified *E. coli* and human H69 constructs titrated with the aminoglycosides. CD ellipticity changed with increasing concentrations of aminoglycoside (Figure 4). Titration of the unmodified *E. coli* H69 with paromomycin increased the ellipticity at low concentrations approximating the $K_d$ of the primary binding site. An increased ellipticity is associated with an increase in stacking and therefore, would be consistent with an increase in the $T_m$ as the RNA is titrated with the aminoglycoside. The affinity of the unmodified *E. coli* H69 for paromomycin as determined from the CD data differed little from that

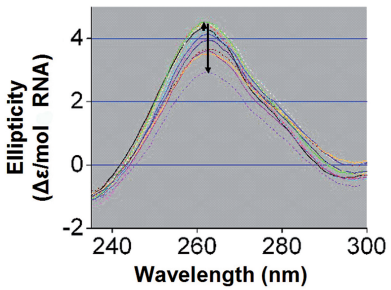


**Figure 4.** Paromomycin binding to the unmodified *E. coli* H69 detected by changes in CD spectra. CD spectra were collected of the unmodified *E. coli* H69 in absence of aminoglycoside (black line) and in the presence of increasing concentrations of paromomycin (0.75–9.00 μM). In this example, the ellipticity increased with increasing concentration of paromomycin at low concentrations (0.75, 1.50 and 2.25 μM; arrow up). At higher concentrations of paromoycin (3.00 4.50, 5.25, 6.00, 6.75, 7.50, 8.25 and 9.00 μM; arrow down), the ellipticity of the RNA decreased.

determined from the thermal denaturation experiments ($K_d$ = 3.5 versus 5.4 μM, respectively). With increasing concentrations of the aminoglycoside, the ellipticity of the CD spectra decreased (Figure 4) and the second site binding constant again approximated that derived from the thermal denaturations, but was higher ($K_d$ = 9.6 versus 6.4 μM, respectively). The human H69 exhibited a weaker affinity for paromomycin than did the *E. coli* H69. The primary binding site had a dissociation constant more than 10-fold higher than that of the unmodified *E. coli* H69 ($K_d$ = 39.6 versus 3.5 μM, respectively). The $K_d$ derived from the CD analysis was consistent with that obtained from the thermal denaturations ($K_d$ = 39.6 versus 35.6 μM, respectively).

## H69 binding of neomycin observed with ITC

ITC determines the change in heat capacity of a macromolecule with the binding of a ligand (38). Thus, the data is a direct measure of energy changes in the system, even for single-stranded RNA (55). In comparison to ITC, changes in an RNA's thermal denaturation with addition of increasing amounts of ligand as determined by UV absorbance are an indirect measure of the energy changes. Though ITC consumes considerable amounts of H69 hairpin, it is complementary to, and confirms other measurements of thermal stability when small ligands are bound by RNAs (56). Therefore, in order to determine if the UV-monitored thermal denaturations

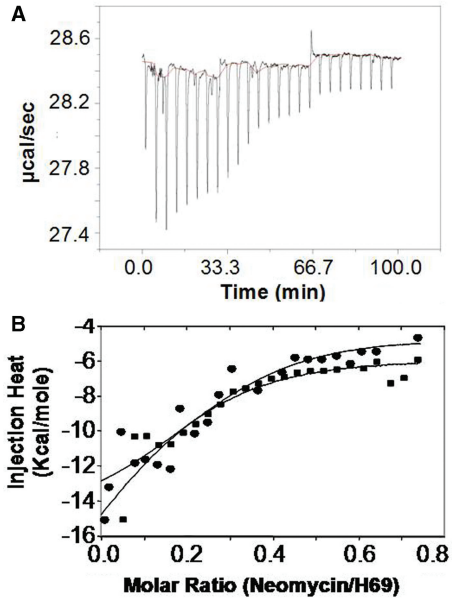


**Figure 5.** ITC of neomycin B binding to the unmodified *E. coli* and human H69 hairpins. The unmodified *E. coli* and human H69 hairpins were titrated with neomycin and the change in heat capacity monitored by ITC. (**A**) Titration of the unmodified *E. coli* H69 with neomycin B as monitored by ITC. The ITC profile for the titration of the unmodified *E. coli* H69 with neomycin B was conducted at 37°C. Each heat burst is the result of a 10 µL injection of 250 µM neomycin. (**B**) Binding of neomycin by the unmodified *E. coli* (filled square) and human H69 RNAs (filled circle). The corrected injection heats (kcal/mol) are derived by integration of the corresponding heat burst curves (A) and corrected for background. The data for the titration of the human H69 has been normalized to that of the *E. coli* H69 in order to plot them on the same graph.

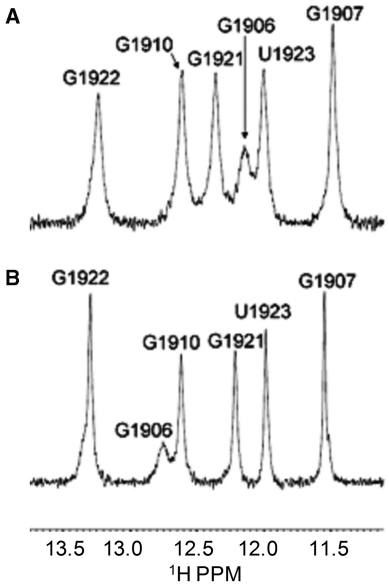


**Figure 6.** Detection of the based paired imino protons of unmodified *E. coli* H69 by NMR. The base-paired, imino proton region of the one-dimensional $^1$H NMR spectra of H69 exhibited six low field shifted resonances between 11.00 and 14.00 ppm: (**A**) H69-neomycin B complex. The line broadening of all resonances and the dramatic chemical shift change of G1906 and G1921 could be observed in comparison to the free H69 (**B**). H69–neomycin B complex. The line broadening of all resonances and the dramatic chemical shift change of G1906 and G1921 could be observed in comparison to the free H69 (B).

were reasonable reflections of the change in heat capacity of the system with the binding of ligand, titrations of the unmodified *E. coli* H69 and the human H69 with neomycin B were monitored by ITC (Figure 5). The binding curves derived from the titrations were found again to be best analyzed as a non-linear, two-site binding. For the unmodified *E. coli* H69, the affinity for neomycin B at the primary binding site was identical to that from the thermal denaturations, $K_d = 0.3 \pm 0.5$ µM. However, the second site affinity for neomycin B was considerably lower than that derived from the thermal denaturations ($K_d = 17.9$ versus 4.3 µM, respectively). In comparison, neomycin B was bound by the human H69 domain with a first site $K_d$ of 55.1 µM, as compared to the 1.5 µM determined by the UV-monitored thermal denaturations. The binding curve derived from the ITC appears to reflect the additional, second site binding, along with the primary site, and an analysis with a two site fitting was not achievable. The free energy of binding of neomycin B by ITC was $\Delta G^\circ_{37} = -6.0$ kcal/mol in comparison to $\Delta G^\circ_{37} = -8.2$ kcal/mol derived from the thermal denaturations (Table 2).

### H69 interaction with neomycin B observed by NMR

The NMR of RNA's base paired imino protons are highly sensitive to changes in dynamics. Therefore, in order to identify and observe the specific nucleosides of H69 that interact with neomycin B, we titrated the *E. coli* unmodified H69 (0.3 mM) with neomycin B (0.1–0.3 mM) and monitored these resonances. As a result, upon complex formation, the imino protons of the residues which are involved in the interaction with neomycin B, should give rise to detectable shifts and considerable line broadening of their corresponding resonances compared to those of the free H69. This allowed us the unambiguous identification of the RNA bases which may be involved in the interaction with neomycin B. The advantage of this approach is that RNA imino proton resonances are typically found at the low field end of the NMR spectrum (57), and thus any changes to them can be selectively monitored without interference from the neomycin B resonances.

Prior to the above-mentioned titration, the imino protons of the free H69 were identified and assigned by using a combination of $^1$H 1D and 2D NOESY NMR experiments run at 2°C and in aqueous solvent (see Materials and Methods section). The results of these experiments yielded six imino proton resonances observed between 11.00 and 14.00 ppm (Figure 6A). The identified peaks were sequentially and specifically assigned by using the cross-peaks observed in the same spectral region of the 2D NOESY spectrum (Figure 7). The two imino protons engaged in the wobble base pair G1907–U1923 were readily identified and assigned due to their distinctive chemical shifts found at 11.62 and 12.06 ppm (Table 3). This preliminary result constituted the starting point for the assignment of G1910, G1921 and G1922

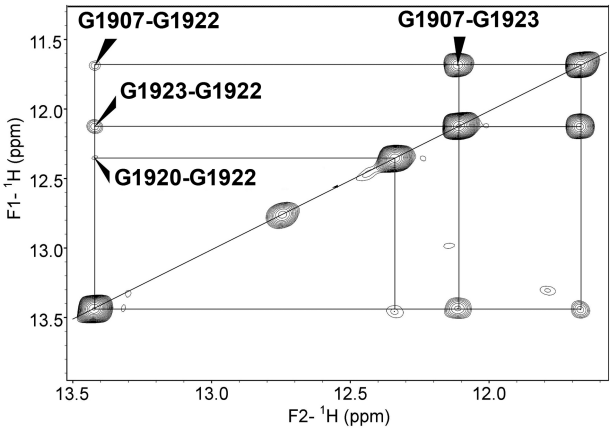


**Figure 7.** $^1$H 2D NOESY spectrum of the unmodified *E. coli* H69. The 2D spectrum is expanded in order to focus on the imino protons resonance region ($F_1$ = 11.00–13.90 ppm; $F_2$ = 11.00–13.50). The sequential NOE connectivities between imino protons in H69 are shown and were used to unambiguously assign the base paired protons.

**Table 3.** NMR titration of *E.coli* unmodified H69 with neomycin

| Residue | Free H69 $\delta_1$ (ppm) | Complex H69–neomycin B $\delta_2$ (ppm) | $\Delta\delta$, $(\delta_2 - \delta_1)$ |
|---|---|---|---|
| G1906 | 12.83 | 12.21 | −0.62 |
| G1907 | 11.62 | 11.56 | −0.06 |
| G1910 | 12.69 | 12.68 | −0.01 |
| G1921 | 12.29 | 12.43 | 0.14 |
| G1922 | 13.37 | 13.31 | −0.06 |
| U1923 | 12.06 | 12.07 | 0.01 |

Chemical shift (δ, ppm) of the imino proton resonances after the addition 1.0 eq. of neomycin. Data based on Figure 6.

imino protons (Figure 7; Table 3). The broad peak observed at 12.83 ppm on the 1D spectrum of the H69 (Figure 6A; Table 3) could not be identified on the NOESY spectrum indicating a fast exchange between the corresponding imino proton and the protons of water. The fast exchange could be due to the fraying of the terminal stem base pair G1906–C1924 and therefore, this resonance was assigned to the G1906 imino proton. The identification and assignment of U1911 imino protons and the non-hydrogen bonded imino protons of the loop residues were prevented by this property of fast exchange (57).

Following the addition of 1.0 equivalent of neomycin B, the resonance intensities of all imino protons broadened (Figure 6B). However, a comparison of the chemical shift of the base pair imino protons in the presence of 0 and 1.0 equivalent of neomycin B displayed some specific and significant differences (Table 3). The result showed that the G1906 base pair imino proton resonance was significantly shifted to the high field by 0.62 ppm and G1921 to the low field by 0.14 ppm. G1907 and G1922 resonances were shifted to the high field by 0.06 ppm whereas the shift for U1923 and G1910 resonance was by 0.01 ppm. The assignment of G1906 was confirmed by using $^1$H 1D NOE difference spectroscopy recorded before and after the titration (Figure 8).

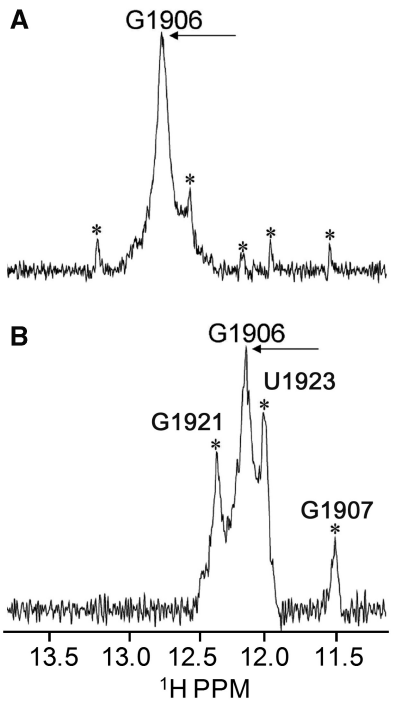


**Figure 8.** *Escherichia coli* unmodified H69 $^1$H 1D NOE difference NMR experiments. (**A**) The G1906 imino proton resonance of the free H69 is irradiated. G1906 and G1910 respective imino proton resonances were found to be in close proximity and as a consequence the irradiation of G1906 imino proton resonance expanded to G1910 and this, in addition to spin diffusion, resulted in the observation of very weak NOE effects between G1906 and all residues. (**B**) The G1906 imino proton resonance of the free H69 is irradiated in the presence of neomycin. Strong NOE effects are observed between G1906 and G1907, U1923 and G1921. Knowing that U1923 is adjacent to G1906, the NOE effect detected between these residues could be partially due to the spillage of G1906 resonance irradiation over the peak of U1923. The observation of an intense NOE between G1906 and the distant peak of G1907 imino proton allow us to conclude that neomycin could have restricted the dynamics of H69 upon H69–neomycin B complex formation. Arrow denotes the irradiated peak and asterisks denote the resulting NOE effects.

## DISCUSSION

Correct ribosome assembly and function are dependent on the Ψ1911, Ψ1915 and Ψ1917 modifications in the loop of the bacterial H69 (58). However, their presence did not contribute appreciably to aminoglycoside binding. We found that paromomycin bound the Ψ-modified *E. coli* H69 with a $K_d$ similar to that of the unmodified RNA. The crystal structures of aminoglycosides bound to the *E. coli* ribosome show that the binding site is located mostly on the 3′-side of the H69 stem and adjacent to the loop with the closest modification, Ψ1917, being 3–4 nucleosides distant (15). In addition, Ψ-modified RNA loops are known to have only subtle differences in their structures and stabilities in comparison to the unmodified RNA (30,31,33,46). Thus, the modifications of the H69, occurring also in the native human H69, may not be factors in the binding of aminoglycosides. At this time, we have not compared the binding of aminoglycosides to the unmodified human H69 to that of the modified.

Human H69 has pseudouridines not only in the terminal loop (nucleosides 3727, 3731, 3733), but also in the stem (3737 and 3739; Figure 1A) (31) at the potential binding site that is analogous to that of the *E. coli* H69. It might be useful in the future to conduct aminoglycoside binding experiments using the modified human H69 to determine if the Ψs influence binding to a greater degree than with the *E. coli* counterpart.

Aminoglycoside antibiotics are known to vary considerably in their binding to RNAs, exhibiting distinctly different affinities that depend on the RNA, and on the conditions (6–8,59). Affinities have been found to vary as much as two orders of magnitude when comparing different RNAs, and even the same RNA but different experimental conditions and methods (60–62). In addition, the finding that the data best fits a two-site binding analysis is not uncommon for model systems (49,50,63,64), as we have found for H69. From the Hill analysis, the binding of aminoglycoside to the primary binding site may provide a conformational change that promotes the secondary binding. However, the second site binding is most likely due to non-specific electrostatic interactions of the positively charged amines of the antibiotic with the RNA backbone, especially in the absence of competing mono- and divalent cations (50). Our studies were conducted in the presence of ~50 mM $Na^+$ far exceeding the 1 μM concentration of the heptadecamer H69 constructs. However, the assay conditions did not include divalent ions ($Mg^{2+}$) with which the aminoglycosides would compete for binding to the RNA backbone, nor changes in pH that appear to affect the structure of the Ψ-modified *E. coli* H69 (65). In the X-ray crystallographic structure (15), the unique aminoglycoside-binding site is in the major groove of H69 at the base of its stem, which would contact the P-site. We hypothesized that the binding of aminoglycosides to the secondary binding site was not observed in the case of the crystal structure as a result of a specific conformation adopted by H69 during crystallization that prevented the observation of a secondary binding site. It is also possible that the interactions between H69 and the P-site could also have an inhibitory effect of the formation of a secondary aminoglycoside-binding site.

The unmodified *E. coli* H69 hairpin bound the four aminoglycoside antibiotics with significantly different affinities (Table 1). Neomycin B and tobramycin were bound by H69 with nanomolar dissociation constants, whereas paromomycin was bound with micromolar $K_d$s (Table 1). Streptomycin was not bound at all. The binding affinities derived from the UV-monitored thermal denaturations were for the most part confirmed by CD and ITC. Larger differences in binding constants were evident with the weaker binding of aminoglycosides to the human H69. The binding mechanism of aminoglycosides is both electrostatic and H-bonding (50,59,64,66,67). Thus, it is no surprise that the highest affinity was exhibited by neomycin B with six amines, five of which would be charged at the pH of the assay (49). Both tobramycin and paromomycin have five amines, of which four would be protonated, and streptomycin has one. RNA affinity for the aminoglycosides tends to heavily relate to the number of amines (14) and is diminished with increasing ionic strength and higher pH of the solution in which they are tested (49,65). Significantly, neomycin B and tobramycin have two amines on each of rings I and II, whereas paromomycin has but one amine on ring I (Figure 1D and E). In contrast, streptomycin has but a methylamine on ring I, and no amine on ring II (Figure 1F). Neither of the *E. coli* nor the human H69 constructs bound streptomycin. Streptomycin-binding aptamers have provided insights into its molecular recognition of RNA in solution and in crystal (68,69). The crystal structure of streptomycin bound to an RNA aptamer revealed that the para- and ortho-substituted guanidinium groups of ring III play critical roles in its molecular recognition of the RNA aptamers. Perhaps, they were unable to do so with the H69 constructs.

These differences in binding altered the $T_m$ of the RNA and were probably enthalpic in origin. Not only were there distinguishing differences among the four aminoglycosides, but binding affinities of the individual antibiotics for the *E. coli* H69 differed from that of the human H69 suggesting that the sequence and conformation of the prokaryotic RNA were more suitable for binding. Paromomycin (as well as other neomycin-class aminoglycosides) protect bases A1408 and G1494 of the bacterial h44 from chemical probes. A1408 is one-third of an adenine platform, also comprised of A1492 and A1493, which helps to stabilize the RNA. The crystal structure of paromomycin bound to the eubacterial A-site confirmed the importance of both nucleotides to the aminoglycoside–RNA interaction (11). Yet, the base re-orientation of A1492 and A1493 associated with the binding of tRNA to h44 is not restricted by the presence of paromomycin (11,70). In comparison, the dynamic character of H69 appears restricted with the binding of aminoglycosides (15). The crystal structures of aminoglycosides binding to *E. coli* H69 demonstrate interactions that mainly employ the G1921, U1923 and the cross strand G1906. Thus, the A-platform found in the terminal loop of H69 does not appear to be involved directly in the binding of aminoglycosides. H69 hairpin sequences with one or more antibiotics could confirm that the aminoglycoside binding to the 3′-side of the stem and do not require the A-platform. Our NMR studies of the unmodified H69 hairpin sequence with neomycin B and under solution conditions identical to those of the UV and CD investigations did confirm that the aminoglycosides bind to the 3′-side of the H69 stem and involve G1906 and G1921.

Aminoglycosides have been used successfully as antibiotics for a long time and are now used also as experimental therapies for cystic fibrosis and Duchenne's muscular dystrophy to counter non-sense mutations (71). However, their penetration of eucaryotic cells is compromised by the amino group positive charges, and can be toxic to humans at high concentrations. Therefore, one would expect they would be ideal broad spectrum antibiotics at low concentrations. Yet, the membranes of gram-positive bacteria prevent uptake, modification enzymes in bacteria alter efficacy and an oxygen-dependent transport system is required, thus negating their use against anaerobic

pathogens (67,71). In addition, the positive charge is a hindrance to uptake by gram-negative bacteria. Bioavailability is reduced by poor oral absorption, but succeeds very well in topical applications. The positively-charged amino groups are attracted to and bind the negatively-charged phosphate backbone of the RNA with an affinity that competes with cations. Still, there is a specificity for RNA structure as demonstrated by the aminoglycoside binding to only two sites on the bacterial ribosome, helix 44 at the decoding site of the small subunit (11), and at the stem and loop of helix 69 of the large subunit at the interface with the small subunit (15). As we have shown, the different aminoglycosides exhibit distinct binding properties for the stem and loop of helix 69 and bind the human counterpart to a lesser degree. Perhaps through alteration of the aminoglycoside structures (67), tobramycin and neomycin uptake and efficacy as antibiotics can be increased while maintaining differential absorption to humans without increasing toxicity.

## SUPPLEMENTARY DATA

Supplementary Data are available at NAR Online.

## ACKNOWEDGEMENTS

The authors wish to thank Dr Jamie Cate for giving suggestions for the manuscript.

## FUNDING

Grants from the National Institutes of Health [GM23037] (to P.F.A.) and the National Science Foundation [MCB0548602]. Funding for open access charge: National Science Foundation.

*Conflict of interest statement*. None declared.

## REFERENCES

1. Moazed,D. and Noller,H.F. (1987) Interaction of antibiotics with functional sites in 16S ribosomal RNA. *Nature*, **327**, 389–394.
2. Magnet,S. and Blanchard,J.S. (2005) Molecular insights into aminoglycoside action and resistance. *Chem. Rev.*, **105**, 477–498.
3. Tor,Y. (2006) The ribosomal A-site as an inspiration for the design of RNA binders. *Biochimie*, **88**, 1045–1051.
4. Misumi,M., Nishimura,T., Komai,T. and Tanaka,N. (1978) Interaction of kanamycin and related antibiotics with the large subunit of ribosomes and the inhibition of translocation. *Biochem. Biophys. Res. Commun.*, **84**, 358–365.
5. Campuzano,S., Vazquez,D., Modolell. and J. (1979) Functional interaction of neomycin B and related antibiotics with 30S and 50S ribosomal subunits. *Biochem. Biophys. Res. Commun.*, **87**, 960–966.
6. Hermann,T. and Westhof,E. (1998) Aminoglycoside binding to the hammerhead ribozyme: a general model for the interaction of cationic antibiotics with RNA. *J. Mol. Biol.*, **276**, 903–912.
7. Raghunathan,D., Sanchez-Pedregal,V.M., Junker,J., Schwiegk,C., Kalesse,M., Kirschning,A. and Carlomagno,T. (2006) TAR-RNA recognition by a novel cyclic aminoglycoside analogue. *Nucleic Acids Res.*, **34**, 3599–35608.
8. Varani,L., Spillantini,M.G., Goedert,M. and Varani,G. (2000) Structural basis for recognition of the RNA major groove in the tau exon 10 splicing regulatory element by aminoglycoside antibiotics. *Nucleic Acids Res.*, **28**, 710–719.
9. Davies,J. and Davis,B.D. (1968) Misreading of ribonucleic acid code words induced by aminoglycoside antibiotics. *J. Biol. Chem.*, **243**, 3312–3316.
10. Lynch,S.R. and Puglisi,J.D. (2001) Structural origins of aminoglycoside specificity for prokaryotic ribosomes. *J. Mol. Biol.*, **306**, 1037–1058.
11. Carter,A.P., Clemons,W.M., Brodersen,D.E., Morgan-Warren,R.J., Wimberly,B.T. and Ramakrishnan,V. (2000) Functional insights from the structure of the 30S ribosomal subunit and its interactions with antibiotics. *Nature*, **407**, 340–348.
12. Vicens,Q. and Westhof,E. (2001) Crystal structure of paromomycin docked into the eubacterial ribosomal decoding A-site. *Structure*, **9**, 647–658.
13. Vicens,Q. and Westhof,E. (2003) Molecular recognition by ribosomal RNA and resistance enzymes: An analysis of x-ray crystal structures. *Biopolymers*, **70**, 42–57.
14. Vicens,Q. and Westhof,E. (2003) Crystal structure of geneticin bound to a bacterial 16S ribosomal RNA A-site oligonucleotide. *J. Mol. Biol.*, **326**, 1175–1188.
15. Borovinskaya,M.A., Pai,R.D., Zhang,W., Schuwirth,B.S., Holton,J.M., Hirokawa,G., Kaji,A. and Cate,J.H. (2007) Structural basis for aminoglycoside inhibition of bacterial ribosome recycling. *Nat. Struct. Mol. Biol.*, **14**, 727–732.
16. Hirokawa,G., Kiel,M.C., Muto,A., Selmer,M., Raj,V.S., Liljas,A., Igarashi,K., Kaji,H. and Kaji,A. (2002) Post-termination complex disassembly by ribosome recycling factor, a functional tRNA mimic. *EMBO J.*, **21**, 2272–2281.
17. Hirokawa,G., Kaji,H. and Kaji,A. (2007) Inhibition of antiassociation activity of translation initiation factor 3 by paromomycin. *Antimicrob. Agents Chemother.*, **51**, 175–180.
18. Weixlbaumer,A., Petry,S., Dunham,C.M., Selmer,M., Kelley,A.C. and Ramakrishnan,V. (2007) Crystal structure of the ribosome recycling factor bound to the ribosome. *Nat. Struct. Mol. Biol.*, **14**, 733–777.
19. Yusupov,M.M., Yusupova,G.Z., Baucom,A., Lieberman,K., Earnest,T.N., Cate,J.H. and Noller,H.F. (2001) Crystal structure of the ribosome at 5.5 Å resolution. *Science*, **292**, 883–896.
20. Schuwirth,B.S., Borovinskaya,M.A., Hau,C.W., Zhang,W., Vila-Sanjurjo,A., Holton,J.M. and Cate,J.H. (2005) Structures of the bacterial ribosome at 3.5 Å resolution. *Science*, **310**, 827–834.
21. Lescoute,A. and Westhof,E. (2006) The interaction networks of structured RNAs. *Nucleic Acids Res.*, **34**, 6587–6604.
22. Hirabayashi,N., Sata,N.S. and Suzuki,T. (2006) Conserved loop sequence of helix 69 in *Escherichia coli* 23S rRNA is involved in A-site tRNA binding and translational fidelity. *J. Biol. Chem.*, **281**, 17203–17211.
23. Liang,X.H., Liu,Q. and Fournier,M.J. (2007) rRNA modifications in an intersubunit bridge of the ribosome strongly affect both ribosome biogenesis and activity. *Mol. Cell*, **28**, 965–977.
24. Kipper,K., Hetényi,C., Sild,S., Remme,J. and Liiv,A. (2009) Ribosomal intersubunit bridge B2a is involved in factor-dependent translation initiation and translational processivity. *J. Mol. Biol.*, **385**, 405–422.
25. O'Connor,M. (2009) Helix 69 in 23S rRNA modulates decoding by wild type and suppressor tRNAs. *Mol. Genet. Genomics*, **282**, 371–380.
26. Gardner,P.P., Daub,J., Tate,J.G., Nawrocki,E.P., Kolbe,D.L., Lindgreen,S., Wilkinson,A.C., Finn,R.D., Griffiths-Jones,S. and Eddy,S.R. (2009) Rfam: updates to the RNA families database. *Nucleic Acids Res.*, **37**, D136–D140.
27. Hobbie,S.N., Kalapala,S.K., Akshay,S., Bruell,C., Schmidt,S., Dabow,S., Vasella,A., Sander,P. and Böttger,E.C. (2007) Engineering the rRNA decoding site of eukaryotic cytosolic ribosomes in bacteria. *Nucleic Acids Res.*, **35**, 6086–6093.
28. Guenther,R.H., Gopal,D.H. and Agris,P.F. (1988) Purification of transfer RNA species by single-step ion-exchange HPLC. *J. Chromatogr.*, **444**, 79–87.
29. Cantor,C.R., Warshaw,M.M. and Shapiro,H. (1970) Oligonucleotide interactions III. Circular dichroism studies of the conformation of deoxynucleotides. *Biopolymers*, **9**, 1059–1077.

30. Meroueh,M., Grohar,P.J., Qiu,J., SantaLucia,J. Jr, Scaringe,S.A. and Chow,C.S. (2000) Unique structural and stabilizing roles for the individual pseudouridine residues in the 1920 region of *Escherichia coli* 23S rRNA. *Nucleic Acids Res.*, **28**, 2075–2083.
31. Sumita,M., Desaulniers,J.P., Chang,Y.C., Chui,H.M., Clos,L. II and Chow,C.S. (2005) Effects of nucleotide substitution and modification on the stability and structure of helix 69 from 28S rRNA. *RNA*, **11**, 1420–1429.
32. Ashraf,S.S., Guenther,R.H., Ansari,G., Malkiewicz,A., Sochacka,E. and Agris,P.F. (2000) Role of modified nucleosides of yeast tRNA(Phe) in ribosomal binding. *Cell Biochem. Biophys.*, **33**, 241–252.
33. Yarian,C.S., Basti,M.M., Cain,R.J., Ansari,G., Guenther,R.H., Sochacka,E., Czerwinska,G., Malkiewicz,A. and Agris,P.F. (1999) Structural and functional roles of the N1- and N3-protons of psi at tRNA's position 39. *Nucleic Acids Res.*, **27**, 3543–3549.
34. Serra,M.J. and Turner,D.H. (1995) Predicting thermodynamic properties of RNA. *Methods Enzymol.*, **259**, 242–261.
35. McDowell,J.A. and Turner,D.H. (1996) Investigation of the structural basis for thermodynamic stabilities of tandem GU mismatches: solution structure of $(rGAGGUCUC)_2$ by two-dimensional NMR and simulated annealing. *Biochemistry*, **35**, 14077–14089.
36. Guenther,R.H., Hardin,C.C., Sierzputowska-Gracz,H. and Agris,P.F. (1992) Magnesium-induced conformational transition in a DNA analog of the yeast $tRNA^{Phe}$ anticodon stem-loop. *Biochemistry*, **31**, 11004–11011.
37. Dao,V., Guenther,R.H. and Agris,P.F. (1992) The Role of 5-methylcytidine in the anticodon arm of yeast $tRNA^{Phe}$: Site-specific $Mg^{2+}$ binding and coupled conformational transition in DNA analogs. *Biochemistry*, **31**, 11012–11019.
38. Feig,A.L. (2007) Applications of isothermal titration calorimetry in RNA biochemistry and biophysics. *Biopolymers*, **87**, 293–301.
39. Delaglio,F., Grzesiek,S., Vuister,G.W., Zhu,G., Pfeifer,J. and Bax,A. (1995) NMRPipe: a multidimensional spectral processing system based on UNIX pipes. *J. Biomol. NMR*, **6**, 277–293.
40. Goddard,T.D. and Kneller,D.G. (2007) *Sparky 3- NMR Assignment and Integration Software*. http://www.cgl.ucsf.edu/home/sparky/. University of California, San Francisco.
41. ACD/SpecManager, version 10.02 (2006), Advanced Chemistry Development Inc., Toronto ON, Canada, http://www.acdlabs.com (20 October 2009, date last accessed).
42. Piotto,M., Saudek,V. and Sklenar,V. (1992) Gradient-tailored excitation for single-quantum NMR spectroscopy of aqueous solutions. *J. Biomol. NMR*, **2**, 661–665.
43. Neuhaus,D. and Williamson,M.P. (1989) The Nuclear Overhauser Effect in Structural and Conformational Analysis. *VCH Publishers Inc.*. New York.
44. Kumar,A., Ernst,R.R. and Wuthrich,K. (1980) A two-dimensional nuclear Overhauser enhancement (2D NOE) experiment for the elucidation of complete proton-proton cross-relaxation networks in biological macromolecules, *Biochem. Biophys. Res. Commun.*, **95**, 1–6.
45. Macura,S. and Ernst,R.R. (1980) Elucidation of cross relaxation in liquids by two-dimensional NMR Spectroscopy, *Mol. Phys.*, **41**, 95–117.
46. Durant,P.C. and Davis,D.R. (1999) Stabilization of the anticodon stem-loop of $tRNA^{Lys,3}$ by an $A^+$-C base-pair and by pseudouridine. *J. Mol. Biol.*, **285**, 115–131.
47. Desaulniers,J.P., Chang,Y.C., Aduri,R., Abeysirigunawardena,S.C., SantaLucia,J. Jr and Chow,C.S. (2008) Pseudouridines in rRNA helix 69 play a role in loop stacking interactions. *Org. Biomol. Chem.*, **6**, 3892–3895.
48. Sengupta,R., Vainauskas,S., Yarian,C., Sochacka,E., Malkiewicz,A., Guenther,R.H., Koshlap,K.M. and Agris,P.F. (2000) Modified constructs of tRNA's TΨC-domain to probe substrate conformational requirements of $m^1A_{58}$ and $m^5U_{54}$-tRNA methyltransferases. *Nucleic Acids Res.*, **28**, 1374–1380.
49. Kaul,M. and Pilch,D.S. (2002) Thermodynamics of aminoglycoside-rRNA recognition: the binding of neomycin-class aminoglycosides to the A site of 16S rRNA. *Biochemistry*, **41**, 7695–7706.
50. Stampfl,S., Lempradl,A., Koehler,G. and Schroeder,R. (2007) Monovalent ion dependence of neomycin B binding to an RNA aptamer characterized by spectroscopic methods. *Chembiochem.*, **8**, 1137–1145.
51. Chen,Y., Sierzputowska-Gracz,H., Guenther,R., Everett,K. and Agris,P.F. (1993) Methyl-5-cytidine is required for cooperative binding of $Mg^{2+}$ and a conformational transition at the anticodon stem-loop of yeast phenylalanine tRNA. *Biochemistry*, **32**, 10249–10253.
52. Agris,P.F., Marchbank,M.T., Newman,W., Guenther,R., Ingram,P., Swallow,J., Mucha,P., Szyk,A., Rekowski,P. and Peletskaya,E. (1999) Experimental models of protein-RNA interaction: isolation and analyses of $tRNA^{Phe}$ and U1 snRNA-binding peptides from bacteriophage display libraries. *J. Protein Chem.*, **18**, 425–435.
53. Gagnon,G., Zhang,X., Agris,P.F. and Maxwell,S.E. (2006) Assembly of the archaeal box C/D sRNP can occur via alternative pathways and requires temperature-facilitated sRNA remodeling. *J. Mol. Biol.*, **362**, 1025–1042.
54. McPike,M.P., Sullivan,J.M., Goodisman,J. and Dabrowiak,J.C. (2002) Footprinting, circular dichroism and UV melting studies on neomycin B binding to the packaging region of human immunodeficiency virus type-1 RNA. *Nucleic Acids Res.*, **30**, 2825–2831.
55. Breslauer,K.J. and Sturtevant,J.M. (1977) A calorimetric investigation of single stranded base stacking in the ribo-oligonucleotide A7. *Biophys. Chem.*, **7**, 205–209.
56. Thomas,J.R., Liu,X. and Hergenrother,P.J. (2006) Biochemical and thermodynamic characterization of compounds that bind to RNA hairpin loops: toward an understanding of selectivity. *Biochemistry*, **45**, 10928–10938.
57. Varani,G., Abdoul-ela,F. and Allain,F.H.-T. (1996) NMR investigation of RNA structure. *Progr. Nucl. Magn. Reson. Spectrosc.*, **29**, 51–127.
58. Gutgsell,N.S., Deutscher,M.P. and Ofengand,J. (2005) The pseudouridine synthase RluD is required for normal ribosome assembly and function in *Escherichia coli*. *RNA*, **11**, 1141–1152.
59. Kaul,M., Barbieri,C.M. and Pilch,D.S. (2005) Defining the basis for the specificity of aminoglycoside-rRNA recognition: A comparative study of drug binding to the A sites of *Esherichia coli* and human rRNA. *J. Mol. Biol.*, **346**, 119–134.
60. Yang,G., Trylska,J., Tor,Y. and McCammon,A. (2006) Binding of aminoglycosidic antibiotics to the oligonucleotide A-site model and 30S ribosomal subunit: Poisson-Boltzmann model, thermal denaturation, and fluorescence studies. *J. Med. Chem.*, **49**, 5478–5490.
61. Means,J.A. and Hines,J.V. (2005) Fluorescence resonance energy transfer studies of aminoglycoside binding to a T box antiterminator RNA. *Bioorg. Med. Chem. Lett.*, **15**, 2169–2172.
62. McPike,M.P., Goodisman,J. and Dabrowiak,J.C. (2002) Footprinting and circular dichroism studies on paromomycin binding to the packaging region of human immunodeficiency virus type-1. *Bioorg. Med. Chem.*, **10**, 3663–3672.
63. Bradrick,T.D. and Marino,J.P. (2004) Ligand-induced changes in 2-aminopurine fluorescence as a probe for small molecule binding to HIV-1 TAR RNA. *RNA*, **10**, 1459–1468.
64. Cowan,J.A., Ohyama,T., Wang,D. and Natarajan,K. (2000) Recognition of a cognate RNA aptamer by neomycin B: quantitative evaluation of hydrogen bonding and electrostatic interactions. *Nucleic Acids Res.*, **28**, 2935–2942.
65. Abeysirigunawardena,S.C. and Chow,C.S. (2008) pH-dependent structural changes of helix 69 from Escherichia coli 23S ribosomal RNA. *RNA*, **14**, 782–792.
66. Wirmer,J. and Westhof,E. (2006) Molecular contacts between antibiotics and the 30S ribosomal particle. *Methods Enzymol.*, **415**, 180–202.
67. Silva,J.G. and Carvalho,I. (2007) New insights into aminoglycoside antibiotics and derivatives. *Curr. Med. Chem.*, **14**, 1101–1119.
68. Wallace,S.T. and Schroeder,R. (1998) In vitro selection and characterization of streptomycin-binding RNAs: recognition discrimination between antibiotics. *RNA*, **4**, 112–123.

69. Tereshko,V., Skripkin,E. and Patel,D.J. (2003) Encapsulating streptomycin within a small 40-mer RNA. *Chem. & Biol.*, **10**, 175–187.
70. Kaul,M., Barbieri,C.M. and Pilch,D.S. (2006) Aminoglycoside-induced reduction in nucleotide mobility at the ribosomal RNA A-site as a potentially key determinant of antibacterial activity. *J. Amer. Chem. Soc.*, **128**, 1261–1271.
71. Hermann,T. (2007) Aminoglycoside antibiotics: old drugs and new therapeutic approaches. *Cell. Mol. Life Sci.*, **64**, 1841–1852.